An Equilibrial Process Zone in Polymeric Materials

A. STOJIMIROVIC,[1] K. KADOTA,[2] and A. CHUDNOVSKY[2,*]

[1]Argonne National Laboratory, Bldg. 212, 9700 South Cass Avenue, Argonne, Illinois 60439; [2]University of Illinois at Chicago, CEMM Dept., P.O.B. 4348, Chicago, Illinois 60680

SYNOPSIS

A process zone at the tip of a fatigue crack grown in polymeric materials has been widely reported. A new method that treats the process zone as an allotropically transformed material is employed for the prediction of the process-zone size. A specific energy of material transformation as well as transformation stress and draw ratio are determined from an independent test on polymer drawing. The prediction of the model with no adjustable parameters appears to be in a good agreement with the experimentally observed process zone for various polyethylenes and polycarbonate.

INTRODUCTION

Propagation of a fatigue crack by first forming a process zone ahead of the crack and then forcing its way through the zone is a well-known phenomena. The Dugdale–Barenblatt model (DBM) is conventionally employed to analyze the process zone.[1,2] The application of the DBM for various polyethylenes seems plausible since the basic features of the model are observed, e.g., the process zone has a thin strip shape[3,4] and has constancy of stress along the process zone.[5] In this paper, we examine the differences between the size of the process zone formed under fatigue and the DBM prediction. The process-zone size is evaluated based on fatigue striations observed on the fracture surface. Recently, Chudnovsky proposed a new model for the process zone,[6,7] which renders the simplicity of the DBM and the same time releases some of its limitations. In this paper, the Chudnovsky model (CM) is employed to analyze the process zone preceding fatigue crack growth in various polyethylenes reported[8] and polycarbonate.

DESCRIPTION OF THE MODEL

The process zone in front of a crack is considered to be a zone of allotropically transformed material. Indeed, in polyethylene or polycarbonate analyzed below, the drawn material of the process zone can be regarded as a second phase since it differs from the original one by its physical properties and is separated by a distinct boundary. A typical process zone formed in front of a fatigue crack is illustrated in Figure 1(a).

Let G be the Gibbs potential of the two-phase system shown in Figure 1(b) and V_{tr} be the domain occupied by the second phase (process zone). For isothermal condition and fixed remote load, an equilibrial process zone, V_{tr}, renders the minimum of G:

$$\left.\frac{\delta G[\sigma_\infty, l, V_{tr}]}{\delta V_{tr}}\right|_{\sigma_\infty=\text{const},l=\text{const}} = 0 \qquad (1)$$

The brackets indicate that G is a functional of the zone V_{tr} and a function of the crack length, l, and the applied stress, σ_∞.

Following Eshelby,[9] the change in Gibbs potential of the system as a result of the migration of the boundary ∂V_{tr} between two phases can be expressed as

$$\delta G = -\int_{\partial V_{tr}} \delta\xi_i (P_{ij}^0 - P_{ij}^{tr}) n_j \, d\Gamma \qquad (2)$$

where P_{ij} is the energy momentum tensor of elasticity (Eshelby tensor) $P_{ij} = f\delta_{ij} - \sigma_{jk}^* u_{k,i}$; f is the

* To whom correspondence should be addressed.

Journal of Applied Polymer Science, Vol. 46, 1051–1056 (1992)
 CCC 0021-8995/92/061051-06

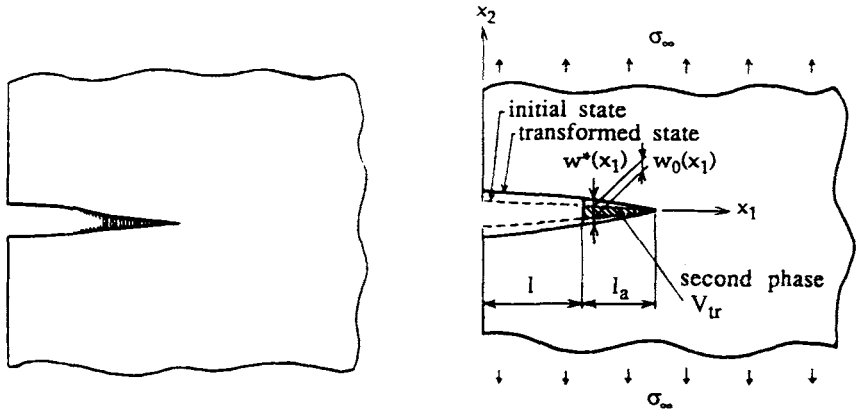

Figure 1 (a) Schematic illustration of the process zone. (b) Schematic illustration of the model.

Helmholtz free-energy density; σ^*_{jk} and $u_{k,i}$ stand for the Piola–Kirchhoff stress tensor and the gradient of the displacement vector u_k, respectively; $\delta\xi_i$ is an infinitesimal vector of boundary migration ∂V_{tr}; and n_j is the unit normal vector directed outward from the transformed toward the initial material. Superscripts "0" and "*tr*" refer to the original and the second (transformed) phase, respectively.

The continuity of the traction and the displacement vectors at the phase boundary ∂V_{tr} and the equilibrium and compatibility equations within each phase together with eq. (1) result in a system of integro-differential equations for determining equilibrial V_{tr}. To our knowledge, there is no analytical solution to the problem in such generality. To simplify the problem, the following assumptions are admitted:

(a) The process-zone width w is much smaller than its length l_a: $w/l_a \ll 1$, i.e., V_{tr} has a shape of a thin strip.

(b) The process zone consists of a cold drawn material with a constant draw ratio, λ.

The two-phase system equilibrium [Fig. 1(b)] is represented as a superposition of the two problems, illustrated in Figure 2. The first results from the original problem after removing the process zone and substituting it with an equivalent traction σ_{tr}. The second is the process zone V_{tr} submitted to σ_{tr} representing the action of the original phase onto the transformed one. The constancy of σ_{tr} along the phase boundary follows from the phase-equilibrium condition.

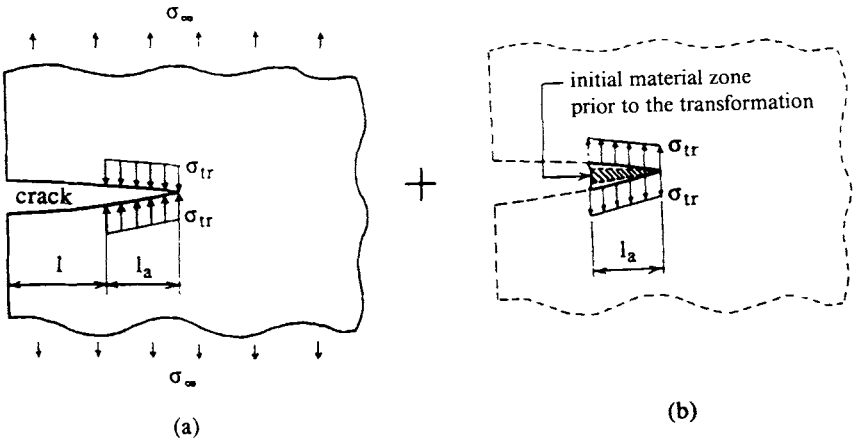

Figure 2 (a) Crack carrying the transformation stress σ_{tr} at its edge and (b) the process zone of the transformed material.

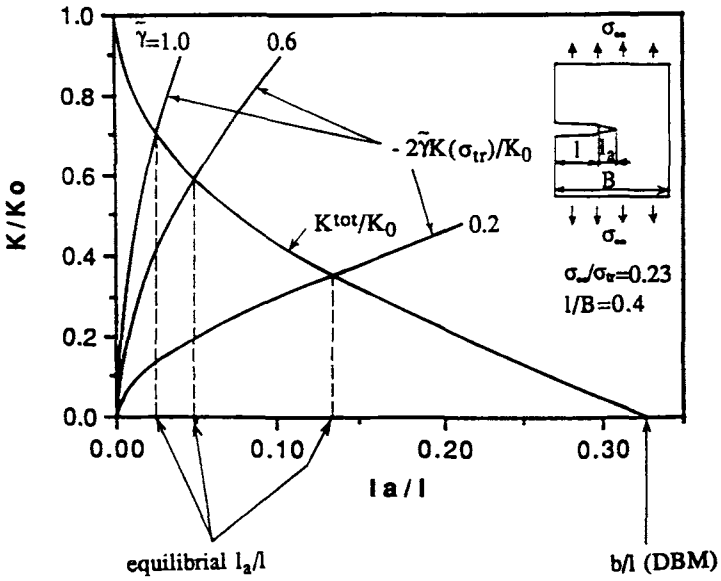

Figure 3 Graphic solution of eq. (8) for various $\tilde{\gamma} = \gamma^{tr}/(\lambda - 1)\sigma_{tr}$ (K_0 is the SIF of the same crack length in absence of the process zone).

The width, w_0, of the layer of the original material that undergoes the transformation varies along the process zone and is unknown. The width, w^*, of the transformed layer is $w^* = \lambda w_0$. The displacement continuity, i.e., the coherency of the phase boundary, can be expressed as follows:

$$w^*(x_1) - w_0(x_1) = \Delta(x_1, l_a) \tag{3}$$

where $\Delta(x_1, l_a)$ stands for the slit-opening displacement [Fig. 2(a)] and x_1 is the coordinate shown in Figure 1(b). Then, the width $w_0(x_1)$ of the initial strip that undergoes the transformation is related to the slit-opening displacement and the draw ratio:

$$w_0(x_1) = \Delta(x_1, l_a)/(\lambda - 1) \tag{4}$$

The volume V_{tr} of the initial material that undergoes the transformation can be expressed as

$$V_{tr} = \frac{t_0}{\lambda - 1}\int_l^{l+l_a} \Delta(l, l_a; \sigma_\infty, \sigma_{tr}; x_1)\, dx_1 \tag{5}$$

where t_0 is the initial thickness of the specimen. Given the assumptions (a) and (b), it can be shown that the variation of V_{tr} is uniquely determined by changes in l_a. Thus, eq. (1) can be rewritten as

$$\left.\frac{dG(\sigma_\infty, l, l_a)}{dl_a}\right|_{\sigma_\infty=\text{const},l=\text{const}} = 0 \tag{6}$$

Since the slit is narrow, we approximate $\Delta(x_1, l_a)$ by the crack-opening displacement (COD) and employing a standard fracture mechanics formalism, eq. (6) leads to the following equation for l_a (Ref. 6):

$$K^{\text{tot}}(\sigma_\infty, \sigma_{tr}; l, l_a)|_{\sigma_\infty=\text{const},l=\text{const}} = -\frac{2\gamma^{tr}}{(\lambda - 1)\sigma_{tr}} K(\sigma_{tr}; l, l_a)\Big|_{l=\text{const}} \tag{7}$$

Here K^{tot} is the stress intensity factor (SIF) for the problem of Figure 2(a), $K(\sigma_{tr}; l, l_a)$ is the SIF for the same problem with absence of σ_∞. A new parameter γ^{tr} ($\equiv P_{22}^0 - P_{22}^{tr}$) represents the jump of the Gibbs potential density (per unit volume) over the boundary between the drawn and original material (see next section).

The three material parameters, γ^{tr}, λ, and σ_{tr} are employed in the model. It should be emphasized that these parameters can be determined in independent tests, e.g., in a tensile test on neck formation, including the heat-flux measurements together with calorimetry for determination of the residual strain energy in the necked region. The evaluation of γ^{tr}, λ, and σ_{tr} for three PEs are presented in the next section.

Figure 3 displays the comparison of the DBM prediction and that of our model for SEN specimen for various $\tilde{\gamma} = \gamma^{tr}/(\lambda - 1)\sigma_{tr}(\sigma_\infty/\sigma_{tr} = 0.23, l/B$

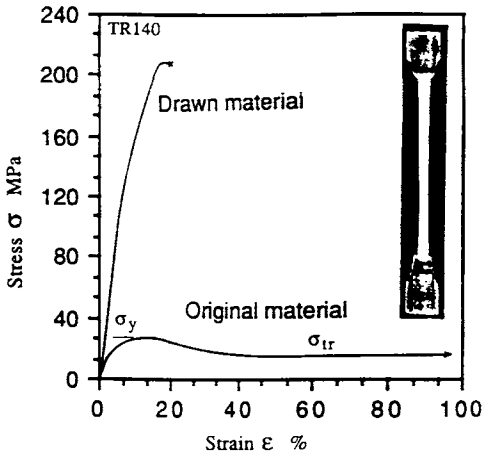

Figure 4 Stress–strain curves of original and drawn material.

= 0.4), where B is a specimen width. The vertical axis is normalized with respect to the SIF K_0 of the same crack in absence of the process zone. $K^{tot} = 0$ gives the DBM process zone length "b" and a point of intersection of two curves (K^{tot} and $-2\tilde{\gamma}K(\sigma_{tr})$) is the equilibrial process-zone length of our model. The equilibrial process-zone length decreases significantly with $\tilde{\gamma}$. For $\tilde{\gamma} \approx 1$, the two models predictions differ by an order of magnitude. It is easy to see from eq. (7) that in the limit $\gamma^{tr}/\sigma_{tr}(\lambda - 1) \rightarrow 0$, the model reduces to the well-known equation of the DBM, i.e., $K^{tot} = 0$.

EVALUATION OF MATERIAL PROPERTIES

The factor $\tilde{\gamma}$ has been measured in a simple tension test.[7] Typical tensile stress–strain curves of initial and drawn PE together with the photograph of a specimen illustrating the growth of a stable neck are shown in Figure 4. The necked material in the tensile test appears as a homogeneously drawn continuum. In contrast, the material within the process zone is highly fibrillated (cavitated) due to the constraint of the plane strain condition. The cavitation and fibrillation are well manifested on the fracture surface and apparently play an important role in the fracture process. For instance, the evolution of micro features on fracture surfaces is directly related to the crack driving force.[10,11] Thus, the value of $\tilde{\gamma}$ obtained in the tensile test with neck formation is simply an approximation of $\tilde{\gamma}$ in a process-zone formation.

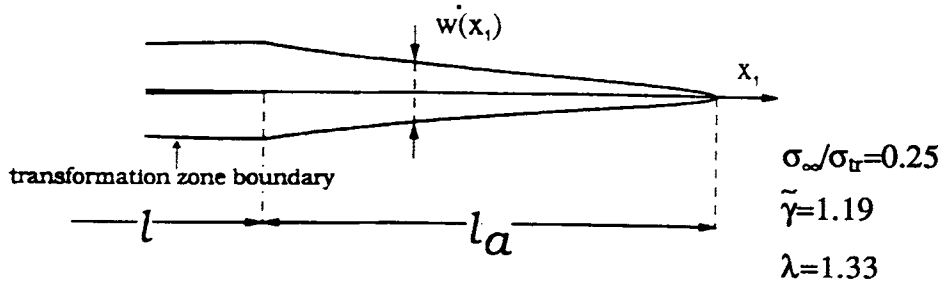

a) The envelope of the process zone (The model prediction).

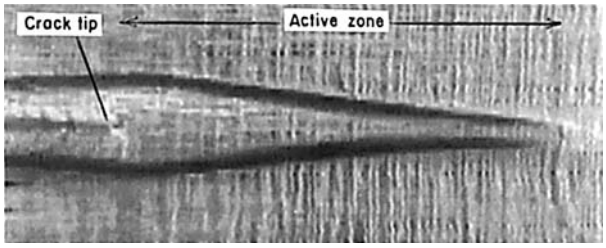

Figure 5 The shape of the process zone. (a) The envelope of the process zone (the model prediction). (b) Composite optical micrograph of a side view of the crack with the process zone in PC.

RESULTS AND DISCUSSION

(a) Shape of the Process Zone

From eqs. (3) and (4), the width of the transformed layer $w^*(x_1)$ can be expressed through the slit opening Δ as $w^*(x_1) = \lambda/(\lambda - 1)\,\Delta(x_1, l, l_a)$. Thus, the shape of the process zone can be uniquely determined by the model for given l and l_a. Figure 5(a) shows the envelope of the set of process zones calculated from the initial crack length to the current crack length. A typical process zone formed in front of a fatigue crack in polycarbonate (PC) is illustrated in Figure 5(b). An effective draw ratio $\lambda^{eff} = 1.33$ was used to account heterogeneous drawing within the process zone.[12] The model prediction shows a very good agreement with that observed experimentally.

(b) Size of the Process Zone

Fatigue striations are observed on the fracture surface.[10] Based on the discontinuous fatigue crack growth mechanism reported elsewhere[8,13] as well as our own observations, we consider the bands between consecutive striations on the fracture surface to be a measure of the corresponding process-zone length. The bandwidth increases with the crack length for every PE studied. The various PEs are distinguished by their branch density.[8] We note that the bandwidth increases with increase in branch density for any given crack length.

Our purpose is to compare the theoretical prediction of the process-zone length, l_a, i.e., the solution of eq. (7) for various l, with the observed bandwidth. The conventional fracture mechanics formalism is employed to evaluate the SIF of eq. (7).

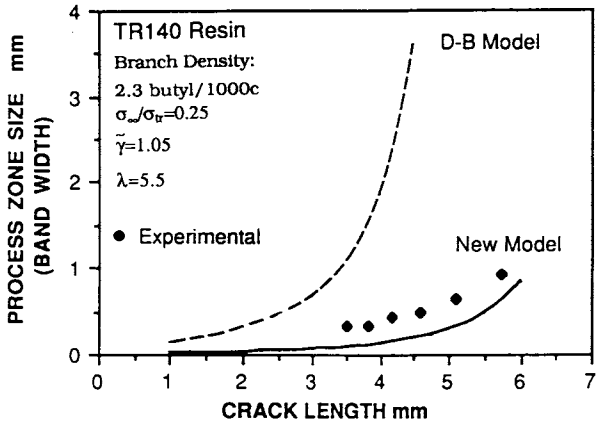

Figure 7 Process zone size vs. crack length (TR1).

The results of an application of the Chudnovsky model (CM) to the three PEs (M5202, TR140, and TR418) are shown in Figures 6, 7, and 8, respectively. The "points" represent the bandwidth observed on the fracture surfaces. The solid lines show the solution of eq. (7) in terms of l_a vs. l. The dashed lines represent the DBM prediction for comparison. The CM gives much better predictions than does the DBM. The predictions are expected to be much better if we account for the cavitation and fibrillation processes and the heat flux. We have observed the exothermic heat flux qualitatively with an IR microscope, but no measurements have been performed yet. Accounting for heat loss leads to a reduction in the reported value of γ^{tr} and, consequently, to an

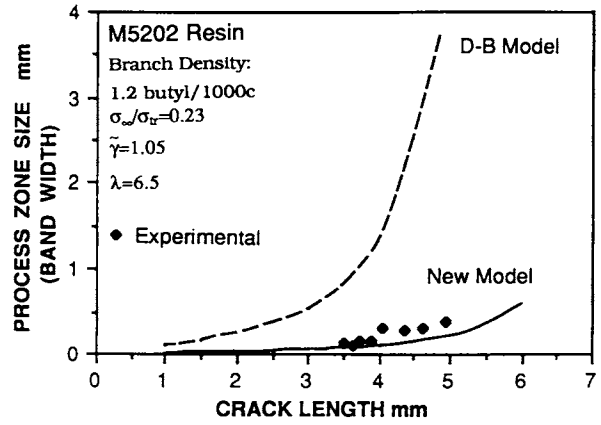

Figure 6 Process zone size vs. crack length (M5202).

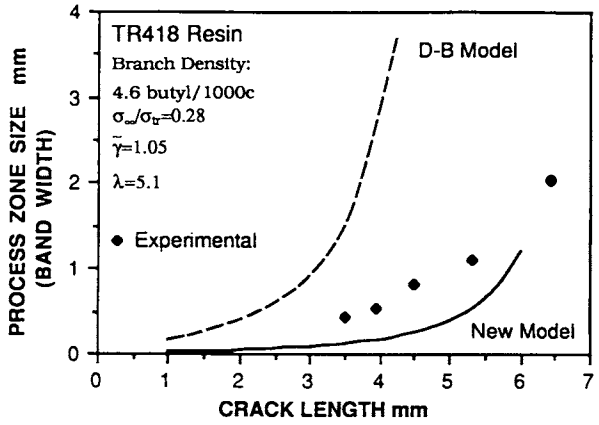

Figure 8 Process-zone size vs. crack length (TR418).

increase in the predicted process-zone size (see Fig. 3).

CONCLUSION

A newly developed model has been successfully applied to describe the characteristics of the process zone ahead of the fatigue crack in polyethylene and polycarbonate. Three material parameters employed in the model can be determined by independent tests. Thus, no adjustable parameters are required. A goal for further studies is to link the material parameters γ^{tr}, λ, and σ_{tr} with the molecular architecture of the polymeric material.

The authors especially wish to thank Prof. N. Brown from the University of Pennsylvania for providing us with the specimens and data of the fatigue test. The financial support from the Gas Research Institute (Contract No. GRI 5088 260 1684) and from the Air Force Office of Science Research (Contract No. FED AFOSR-89-0105) are greatly appreciated. We would like to thank Dr. C. P. Bosnyak and Dr. K. Sehanobish from the Dow Chemical Co., and Prof. A. Moet from Case Western Reserve University for useful discussions and helpful suggestions. The authors also wish to acknowledge the Electron Microscope Facility of the Research Resources Center, University of Illinois at Chicago, for their assistance in conducting this study.

REFERENCES

1. N. Brown and S. K. Bhattacharya, *J. Mater. Sci.*, **20,** 4553 (1985).
2. X. Lu, X. Wang, and N. Brown, *J. Mater. Sci.*, **23,** 643 (1988).
3. K. Chaoui, A. Chudnovsky, and A. Moet, *J. Mater. Sci.*, **22,** 3873 (1987).
4. X. Lu and N. Brown, *J. Mater. Sci.*, **21,** 4081 (1986).
5. X. Wang and N. Brown, *Polymer*, **30,** 1456 (1989).
6. A. Stojimirovic and A. Chudnovsky, to appear.
7. K. Kadota and A. Chudnovsky, in *Proceedings of the ASME Winter Annual Meeting,* Atlanta, GA, Dec. 1–6, 1991, MD-29, p. 101.
8. Y. Zhou, Y. Huang, X. Lu, and N. Brown, in *Plastic Fuel Gas Pipe Symposium Proceedings,* San Francisco, CA, 1989.
9. J. D. Eshelby, in *Inelastic Behavior of Solids,* McGraw-Hill, New York, 1970, p. 77.
10. K. Kadota, A. Chudnovsky, J. Strebel, and A. Moet, in *Proceedings of ANTEC'91,* Montreal, Canada, 1991, p. 2180.
11. K. Sehanobish, A. Moet, A. Chudnovsky, and P. P. Petro, *J. Mater. Sci. Lett.*, **4,** 890 (1985).
12. A. Kim, L. V. Garrett, C. P. Bosnyak, and A. Chudnovsky, *J. Appl. Polym. Sci.*, to appear.
13. J. J. Strebel, private communication, 1990.

Received October 13, 1991
Accepted January 6, 1992